

patterns, which are normalized to their maximum values, have a tendency to form dipole-like shapes and omnidirectional patterns in the E - and H -planes. These plots indicate that the measured radiation patterns have good characteristics. The measured average gain (efficiency) of the proposed antenna is shown in Figure 5. By toggling the PIN diode ON/OFF mode, a significant improvement of the measured frequency responses of the average gain (efficiency) is achieved.

4. CONCLUSION

A frequency reconfigurable PIFA using a PIN diode has been proposed in this article. Despite having a simple structure, the proposed antenna can concurrently cover various bands, including LTE, GSM850, GSM900, DCS, PCS, and UMTS. The simulated and measured results for reflection coefficient, radiation patterns, and average gain (efficiency) showed good characteristics over all bands. As a result, the proposed antenna meets our requirements and is suitable to be adapted for use in wireless mobile phone applications.

ACKNOWLEDGMENT

This research was supported by Basic Science Program Foundation of Korea (NRF) funded by the Ministry of Education, Science and Technology (2011-0005528) and Industry Core Technology Development Project by the Ministry of Knowledge Economy.

REFERENCES

1. J.-B. Yan and J. T. Bernhard, Design of a MIMO dielectric resonator antenna for LTE femtocell base stations, *IEEE Trans Antennas Propag* 60 (2012), 438–444.
2. S. Jeon, Y. Liu, S. Ju, and H. Kim, PIFA with parallel resonance feed structure for wideband operation, *Electron Lett* 47 (2011), 1263–1265.
3. A. Cabedo, J. Anguera, C. Picher, M. Ribo, and C. Puente, Multi-band handset antenna combining a PIFA, slots, and ground plane modes, *IEEE Trans Antennas Propag* 57 (2009), 2526–2533.
4. A. Clemente, L. Dussopt, R. Sauleau, P. Potier, and P. Pouliguen, 1-bit reconfigurable unit cell based on PIN diodes for transmit-array applications in X-band, *IEEE Trans Antennas Propag* 60 (2012), 2260–2269.
5. M.-I. Lai, T.-Y. Wu, J.-C. Hsieh, C.-H. Wang, and S.-K. Jeng, Design of reconfigurable antennas based on an L-shaped slot and PIN diodes for compact wireless devices, *IET Microwave Antennas Propag* 3 (2009), 47–54.
6. Y. Sung, Compact quad-band reconfigurable antenna for mobile-phone applications, *Electron Lett* 48 (2012), 977–979.

© 2013 Wiley Periodicals, Inc.

SMALL-SIZE PLANAR LTE/WWAN ANTENNA AND ANTENNA ARRAY FORMED BY THE SAME FOR TABLET COMPUTER APPLICATION

Kin-Lu Wong, Huan-Jynu Jiang, and Teng-Wei Weng
Department of Electrical Engineering, National Sun Yat-sen University, Kaohsiung 80424, Taiwan; Corresponding author: wongkl@ema.ee.nsysu.edu.tw

Received 23 December 2012

ABSTRACT: For eight-band LTE/WWAN operation (704–960/1710–2690 MHz) in the Ultrabook or thin-profile tablet computer, a planar antenna of simple structure and small size is presented. The proposed

antenna is obtained by modifying a simple planar inverted-F antenna and can be printed on one surface of a thin FR4 substrate of size $10 \times 45 \text{ mm}^2$ only. The antenna's lower band bandwidth is greatly widened by embedding a proper chip capacitor of 2.7 pF at the feeding strip. This chip capacitor combines with the antenna's shorting strip can control the excitation of a parallel resonance to modify the impedance matching of the antenna's lower band such that a widened bandwidth is easily obtained to cover the LTE700/GSM850/900 operation. Conversely, the antenna's upper-band bandwidth is also greatly enhanced by using a coupled section in the antenna's radiating strip and adding a parasitic shorted strip near the feeding strip, which lead to multiple resonant modes excited to form a wide bandwidth ($>1 \text{ GHz}$) to cover the GSM1800/1900/UMTS/LTE2300/2500 operation. Owing to its small size and simple structure, the proposed antenna is very suitable to be applied in achieving an antenna array with high isolation for MIMO or dual talk (dual WWAN) operation. Promising high-isolation antenna arrays formed by the proposed antennas are presented. The obtained isolation between the antennas in the antenna array is better than 12 dB, and the envelope correlation coefficient is less than 0.15 for frequencies over the LTE/WWAN bands. Details of the proposed antenna and antenna array are presented. © 2013 Wiley Periodicals, Inc. *Microwave Opt Technol Lett* 55:1928–1934, 2013; View this article online at wileyonlinelibrary.com. DOI 10.1002/mop.27725

Key words: mobile antennas; tablet computer antennas; LTE/WWAN antennas; antenna array; small-size antennas

1. INTRODUCTION

For applications in the Ultrabook or thin-profile tablet computers, the embedded antennas with planar structure and small size are demanded such that they can be disposed at very limited space therein. For the long-term evolution/wireless wide area network (LTE/WWAN) operation in the 704–960/1710–2690 MHz bands, the demands of planar structure and small size for the embedded antennas are very challenging, especially when at least two LTE/WWAN antennas with high isolation there between are required to be embedded in the limited space inside the tablet computer for LTE multiple-input–multiple-output (MIMO) or dual talk (dual WWAN) operation. Many LTE/WWAN antennas that have been reported for the tablet computers or conventional laptop computers show a three-dimensional structure [1–6] and their occupied antenna volumes range from about $10 \times 55 \times 4 \text{ mm}^3$ [1] to $10 \times 80 \times 3.6 \text{ mm}^3$ [4], which makes these reported antennas less attractive for thin-profile tablet computer applications. Some planar LTE/WWAN antennas suitable to be printed on a thin dielectric substrate to have a thin profile have also been reported recently [7–12], and the antenna's footprint requires from about $11.2 \times 96 \text{ mm}^2$ [12] to about $10 \times 60 \text{ mm}^2$ [8] to cover the LTE/WWAN bands. When considering that at least two LTE/WWAN antennas are required to be embedded in modern mobile devices to perform LTE MIMO operation or for dual talk (dual WWAN) function, the planar LTE/WWAN antennas have a smaller size than the reported ones [7–12] are still demanded. In addition, the antenna structure for achieving wideband or multiband operation should be as simple as possible, which can lead to simple coupling mechanism between such two antennas for frequencies over all the operating bands. This will make it relatively convenient in obtaining good isolation between the antennas of the antenna array formed using the same.

In this article, a small-size planar LTE/WWAN antenna and an antenna array formed using the same for thin-profile tablet computer application is presented. The proposed antenna is suitable to be printed on one surface of a 0.8-mm-thick FR4 substrate

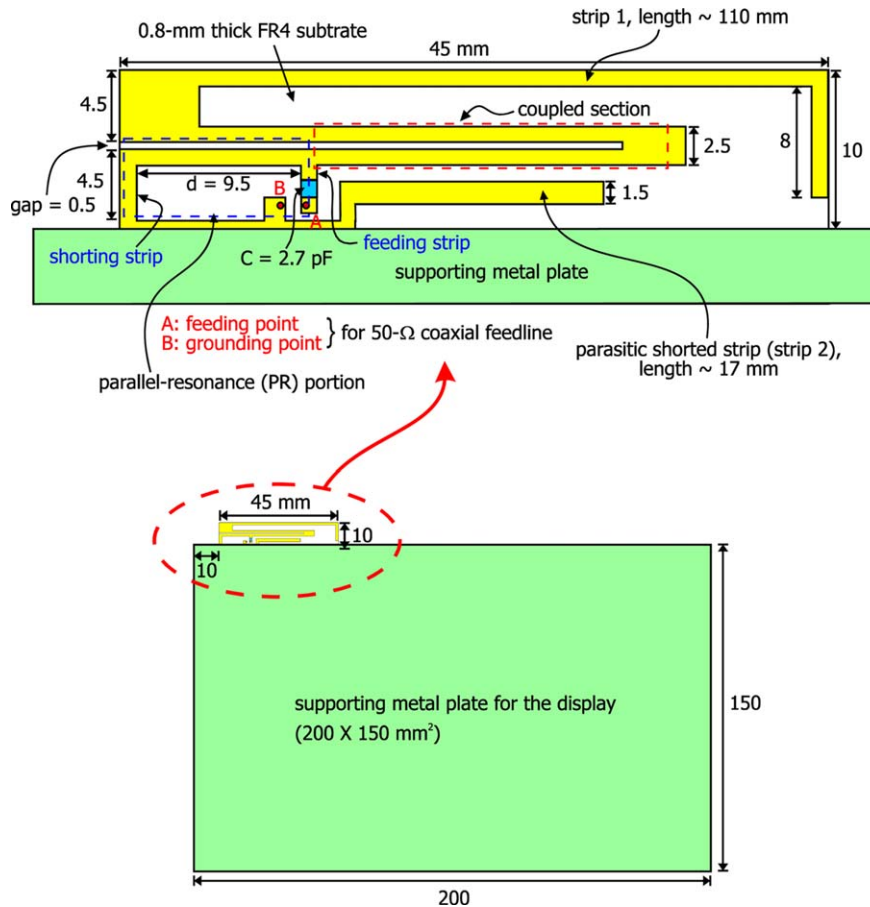


Figure 1 Geometry of the proposed small-size planar LTE/WWAN antenna for tablet computer application (the antenna along the longer edge and near a corner of the supporting metal plate for the display, denoted as antenna 1 in this study). [Color figure can be viewed in the online issue, which is available at www.interscience.wiley.com]

of size $10 \times 45 \text{ mm}^2$ only. Further, the antenna has a simple structure and is obtained by modifying a simple planar inverted-F antenna (PIFA). It is found that the antenna's lower band can be greatly enhanced by simply adding a proper chip capacitor at the antenna's feeding strip, while the antenna's upper band can also be greatly enhanced by forming a coupled section in the antenna's radiating strip and adding a short parasitic shorted strip. The antenna's lower and upper bands can, respectively, cover the desired 704–960 MHz and 1710–2690 MHz for the LTE700/GSM850/900 and GSM1800/1900/UMTS/ LTE2300/2500 operations. The bandwidth-enhancement techniques applied for the proposed antenna to achieve eight-band LTE/WWAN operation will be analyzed. In addition, owing to the small size and simple structure of the proposed antenna, it is very attractive to be applied in forming an antenna array with high isolation for MIMO or dual talk (dual WWAN) operation. Promising high-isolation antenna arrays formed by the proposed antennas are presented. Experimental studies are also conducted, and the obtained isolation between the antennas in the antenna array is better than 12 dB for frequencies over the LTE/WWAN bands. The envelope correlation coefficient less than 0.15 over the LTE/WWAN bands is also obtained. Details of the proposed antenna and the antenna array formed using the same are presented.

2. PROPOSED ANTENNA

The geometry of the proposed small-size planar LTE/WWAN antenna for tablet computer application is shown in Figure 1.

The antenna is mounted along the longer edge and is near a corner of the supporting metal plate for the display. This antenna arrangement is denoted as antenna 1 in this study. Note that the supporting metal plate is selected to have a size of $200 \times 150 \text{ mm}^2$, which are reasonable dimensions for a 9.7-inch tablet computer. The antenna has a planar structure of length 45 mm and height 10 mm above the top edge of the supporting metal plate and is printed on one surface of a 0.8-mm thick FR4 substrate of size $45 \times 10 \text{ mm}^2$, relative permittivity 4.4, and loss tangent 0.024. The antenna is mainly formed by a PIFA with a 2.7-pF chip capacitor embedded at the antenna's feeding strip and a coupled section formed in the antenna's radiating strip (denoted as strip 1 in the figure). A short parasitic shorted strip of length about 17 mm (strip 2 in the figure), which does not increase the size of the antenna, is also added near the antenna's feeding strip to provide an additional resonant mode at about 2.6 GHz to widen the bandwidth of the antenna's upper band.

First, note that the chip capacitor at the feeding strip combines with the antenna's shorting strip to form a parallel-resonance (PR) portion, which can control the impedance property of an excited parallel resonance [13,14] at about 1.4 GHz so as to modify the impedance matching of the antenna's lower band nearby. In the proposed design, a wide operating band to cover the desired 704–960 MHz band for the LTE700/GSM850/900 operation is obtained. In the PR portion, the shorting strip is short-circuited to the supporting metal plate, and the length d is the distance between the shorting strip and the feeding strip. By varying the length d , the excitation of the parallel resonance can

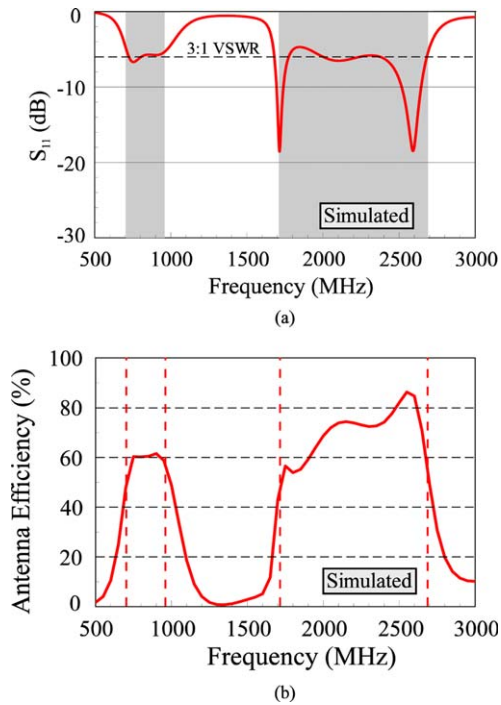


Figure 2 (a) Simulated reflection coefficient S_{11} and (b) antenna efficiency (mismatching losses included) of antenna 1. [Color figure can be viewed in the online issue, which is available at wileyonlinelibrary.com]

be fine-adjusted to fine-tune the impedance matching of the antenna's lower band such that the desired wide operating band is obtained.

For the coupled section in strip 1 of length about 110 mm, it has a long section with a gap of 0.5 mm. This long coupled section can cause increased coupling between the antenna's higher order resonant modes. This is mainly because, along the long coupled section, the higher order resonant modes will have null surface currents, at which strong electric fields will occur. Hence, strong coupling for the antenna's higher order resonant modes can be expected, which can cause the first and second higher-order resonant modes of strip 1 to occur at close frequencies (one at about 1.7 GHz and another at about 2.1 GHz in this study) to form a wider operating band. By further combining the resonant mode contributed by the parasitic shorted strip, a very wide bandwidth of larger than 1 GHz can be obtained for the antenna's upper band to cover the desired 1710–2690 MHz for the GSM1800/1900/UMTS/LTE2300/2500 operation.

To show the results of the proposed antenna in Figure 1 (antenna 1), Figure 2 shows the simulated reflection coefficient S_{11} and antenna efficiency (mismatching losses included). The simulated results are obtained using the three-dimensional full-wave electromagnetic field simulator HFSS version 14 [15]. It can be seen in Figure 2(a) that two wide operating bands are obtained and acceptable impedance matching (better than about 3:1 VSWR or $S_{11} = -6$ dB) is obtained for frequencies over the desired operating bands of 704–960 and 1710–2690 MHz (the shaded frequency regions in the figure). In Figure 2(b), the antenna efficiency is about 60% over the antenna's lower band and ranges about 55–86% over the antenna's upper band. Note that the lowest antenna efficiency of about 55% is seen at about 1.8 GHz at which the impedance matching is about -5 dB (S_{11}), and such antenna efficiencies are still good for practical applications. It is generally acceptable for practical applications,

when the antenna efficiency of the embedded antenna is at least about 40% [16,17].

Effects of the parasitic shorted strip can be seen clearly in Figure 3, in which the simulated S_{11} of antenna 1 with and without strip 2 (parasitic shorted strip) is shown. A resonant mode occurred at about 2.6 GHz is contributed by strip 2, which combines with two higher order resonant modes of strip 1 at about 1.7 and 3.1 GHz to form a very wide operating band to cover the desired 1710–2690 MHz band. The wide lower band covering the desired 704–960 MHz band is contributed by strip 1 excited at its fundamental mode and the PR portion that greatly enhances the lower-band bandwidth.

Effects of the length d in the PR portion are also analyzed. Figure 4 shows the simulated S_{11} [Fig. 4(a)] and input impedance (solid curves for real part and dashed curves for imaginary part) [Fig. 4(b)] of antenna 1 for the length d varied from 7.5 to 11.5 mm. As seen in Figure 1, the length d is the distance between the feeding strip and the shorting strip. When a larger length d is selected ($d = 11.5$ mm in the figure), the excited parallel resonance will occur at closer frequencies to the fundamental resonant mode of strip 1. This behavior will cause large variations in the impedance of the fundamental resonant mode and hence degrade the impedance matching thereof. By selecting a proper length ($d = 9.5$ mm in the figure), a dual-resonance for the antenna's lower band can be obtained, which greatly widens the bandwidth of the antenna's lower band. Conversely, when a smaller length d is selected ($d = 7.5$ mm in the figure), the excited parallel resonance will occur at closer frequencies to the higher order resonant modes of strip 1 and cause large effects on the impedance matching thereof. In this case, the obtained bandwidth of the antenna's upper band is greatly decreased.

Effects of the chip capacitor in the PR portion are shown in Figure 5, in which the simulated S_{11} [Fig. 5(a)] and input impedance (solid curves for real part and dashed curves for imaginary part) [Fig. 5(b)] of antenna 1 for the chip capacitor C varied from 1.5 to 3.9 pF are presented. It is seen that when a proper C (1.5 pF shown in the figure) is selected, good impedance matching for both the lower and upper bands are observed. However, when a smaller C is chosen, the lower-band bandwidth is quickly decreased, and degraded impedance matching for frequencies over the upper band is also seen. Conversely, when a larger C is chosen, the lower-band bandwidth is also decreased, although small effects on the impedance matching for frequencies over the upper band are observed. The results indicate that choosing a proper C is important for the proposed antenna, which can lead to good impedance matching obtained for frequencies over the desired lower and upper bands.

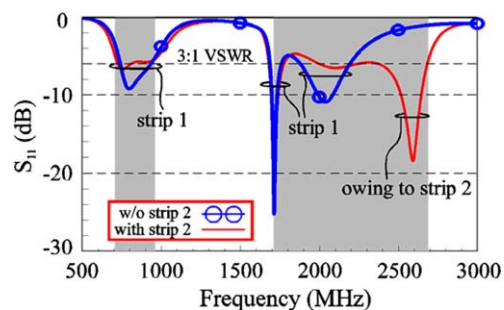
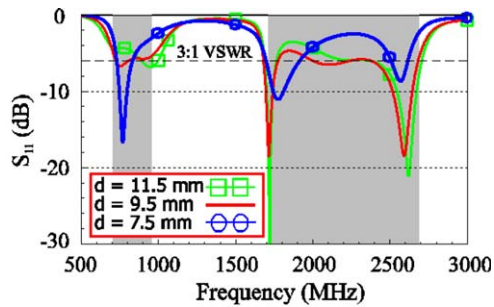
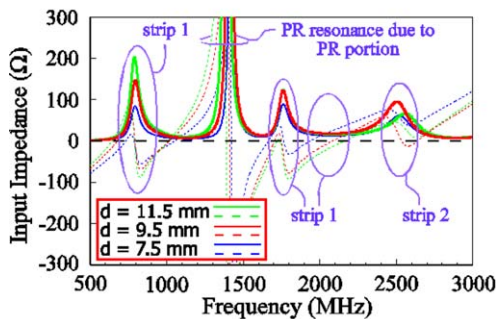


Figure 3 Simulated S_{11} of antenna 1 with and without strip 2 (parasitic shorted strip). [Color figure can be viewed in the online issue, which is available at www.interscience.wiley.com]



(a)

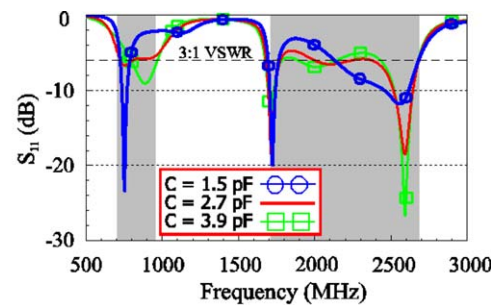


(b)

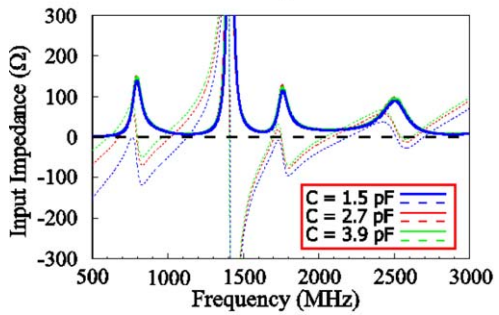
Figure 4 Simulated (a) S_{11} and (b) input impedance (solid curves for real part and dashed curves for imaginary part) of antenna 1 as a function of length d . [Color figure can be viewed in the online issue, which is available at www.interscience.wiley.com]

3. ANTENNA ARRAY FORMED USING THE PROPOSED ANTENNA

Promising antenna arrays formed using the proposed antenna are studied. One promising antenna array (array I) is shown in the inset of Figure 6, in which two proposed antennas (antenna 1 in

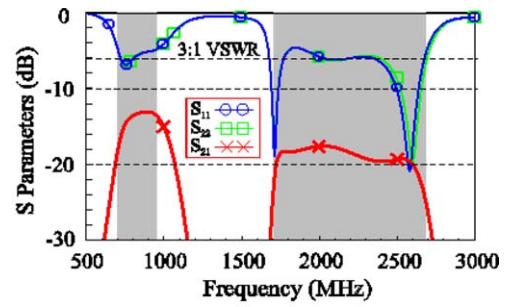


(a)

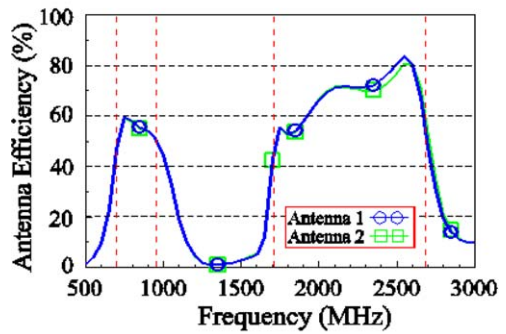


(b)

Figure 5 Simulated (a) S_{11} and (b) input impedance (solid curves for real part and dashed curves for imaginary part) of antenna 1 as a function of chip capacitor C . [Color figure can be viewed in the online issue, which is available at www.interscience.wiley.com]



(a)



(b)

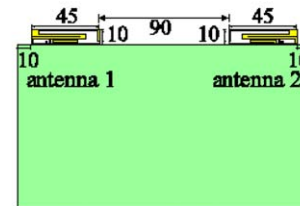
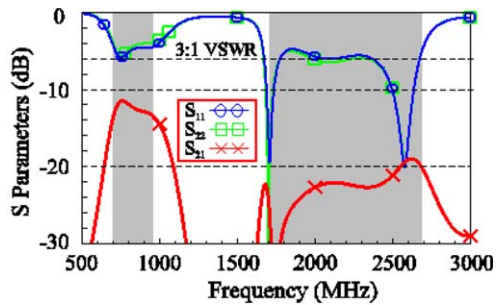


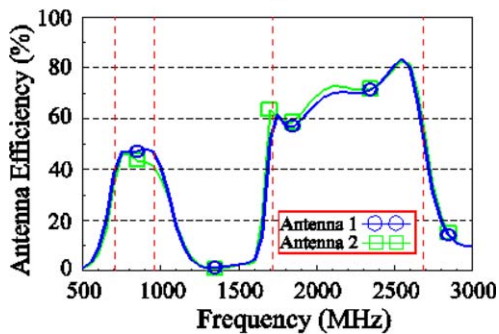
Figure 6 (a) Simulated S parameters of the antenna array formed by antenna 1 mounted near one corner as shown in Figure 1 and antenna 2 mounted near the opposite corner of the longer edge of the supporting metal plate (array I). Dimensions of antenna 2 are the same as those of antenna 1. (b) Simulated antenna efficiency (mismatching losses included) of antennas 1 and 2. [Color figure can be viewed in the online issue, which is available at www.interscience.wiley.com]

Fig. 1 and antenna 2 with same dimensions as antenna 1) are mounted at opposite corners of the longer edge of the supporting metal plate. Figure 6(a) shows the simulated S parameters of the antenna array, and Figure 6(b) shows the simulated antenna efficiency (mismatching losses included) of antennas 1 and 2. Note that owing to the small size of the proposed antenna, the distance between the two antennas is as large as 90 mm, although there is limited space in the tablet computer. In this case, small effects on S_{11} and S_{22} are observed, and the impedance matching of antenna 1 and 2 for frequencies over the lower and upper bands is generally about the same as seen in Figure 2 for the antenna standalone. For the coupling or isolation between two antennas, it is seen that S_{21} over the lower and upper bands is respectively less than -13 and -17 dB, which are good for practical applications [18]. The antenna efficiencies of antenna 1 and 2 are also seen to be about the same as those of the antenna standalone [see Fig. 2(b)], except that the antenna efficiencies over the lower band are about 50–60% which is slightly less than about 60% seen in Figure 2(b).

Another promising antenna array (array II) as seen in Figure 7 is also studied. The two antennas (antenna 1 in Fig. 1 and antenna 3 with same dimensions as antenna 1) are mounted at two adjacent edges of one corner of the supporting metal plate as shown in the inset of Figure 7. Figure 7(a) shows the



(a)



(b)

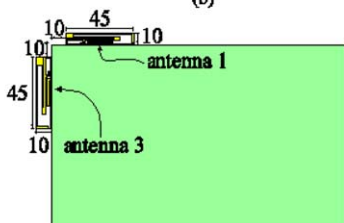
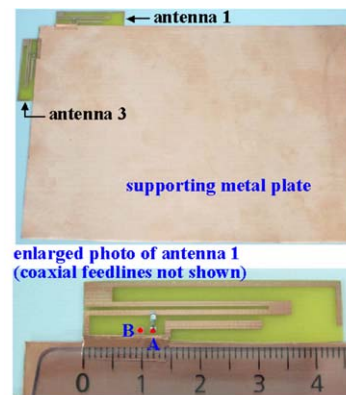


Figure 7 (a) Simulated S parameters of the antenna array formed by antenna 1 mounted as shown in Figure 1 and antenna 3 mounted along the shorter edge and near a corner of the supporting metal plate (array II). Dimensions of antenna 3 are the same as those of antenna 1. (b) Simulated antenna efficiency (mismatching losses included) of antennas 1 and 3. [Color figure can be viewed in the online issue, which is available at www.interscience.wiley.com]

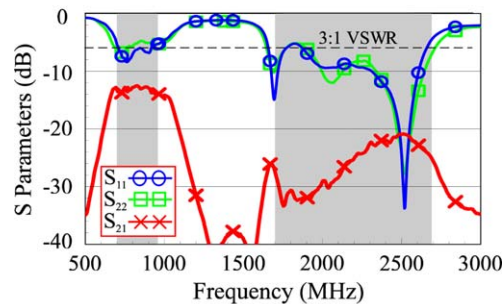
simulated S parameters of the antenna array, and Figure 7(b) shows the simulated antenna efficiency (mismatching losses included) of antenna 1 and 3. In this case, the two antennas are close to each other. Owing to small spacing between the two antennas which causes increased coupling, some degradation on S_{11} and S_{22} for frequencies over the lower band is seen, as compared with the results of the antenna standalone shown in Figure 2(a). The antenna efficiencies over the lower band are seen to be about 40–48% [Fig. 7(b)], which is also smaller than the results for the antenna standalone shown in Figure 2(b). However, with antenna efficiencies better than 40%, it is still acceptable for practical applications in the lower band of about 700–960 MHz [16,17]. For frequencies over the upper band, very small effects on S_{11} , S_{22} , and antenna efficiency are seen. For S_{21} , it is less than about -11 and -19 dB, respectively, over the lower and upper bands, which are still acceptable for practical applications [18]. The obtained results indicate that the antenna array shown in Figure 7 is promising for practical applications and will be experimentally studied.

4. EXPERIMENTAL STUDIES AND DISCUSSION

The antenna array (array II) shown in Figure 7 was fabricated and tested. The photos of the fabricated array II are shown in



(a)



(b)

Figure 8 (a) Photo of the fabricated prototype of array II in Figure 7. (b) Measured S parameters of the fabricated array II. [Color figure can be viewed in the online issue, which is available at www.interscience.wiley.com]

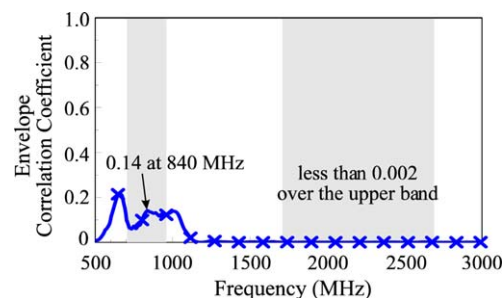


Figure 9 Envelop correlation coefficient ρ_e obtained from measured S parameters of array II in Figure 7(b). [Color figure can be viewed in the online issue, which is available at www.interscience.wiley.com]

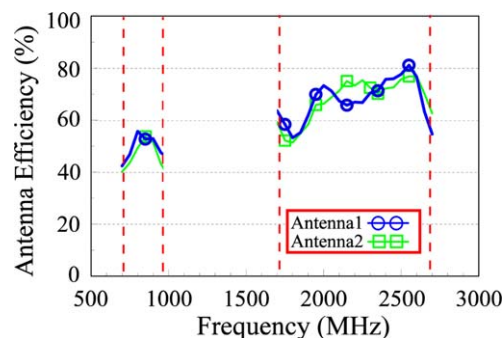


Figure 10 Measured antenna efficiency (mismatching losses included) of antennas 1 and 3 of array II. [Color figure can be viewed in the online issue, which is available at www.interscience.wiley.com]

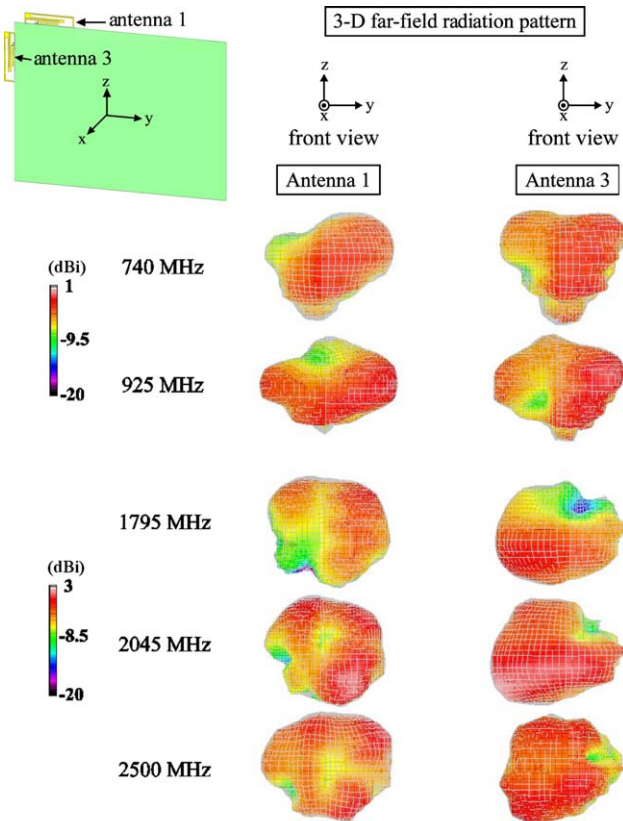


Figure 11 Measured radiation patterns of antennas 1 and 3 of array II. [Color figure can be viewed in the online issue, which is available at www.interscience.wiley.com]

Figure 8(a), and the measured S parameters are shown in Figure 8(b). The measured S_{11} , S_{22} , and S_{21} are similar to the simulated results shown in Figure 7. The measured S_{21} is less than -12 and -21 dB over the lower and upper bands, respectively. The envelop correlation coefficient ρ_e obtained from the measured S parameters [18,19] in Figure 7(b) is shown in Figure 9. It is seen that the envelop correlation coefficient is less than 0.14 over the lower band and is generally very close to 0 over the upper band. The obtained results are very good for practical MIMO applications [18].

Figure 10 shows the measured antenna efficiency (mismatching losses included) of antennas 1 and 3 of the fabricated array II. The antenna efficiencies are also seen to agree with the simulated results shown in Figure 7(b). The antenna efficiencies are about 40–55% and 52–81% over the lower and upper bands, respectively. The measured three-dimensional radiation patterns of antennas 1 and 3 of array II are plotted in Figure 11. For antenna 3, it is seen that strong radiation is seen in the $+y$ direction at lower frequencies (740 and 925 MHz), while at higher frequencies (1795, 2045, and 2500 MHz), strong radiation is generally directed to the $-y$ direction. This behavior suggests that the supporting metal plate with the excited surface currents thereon also contributes to the radiation at lower frequencies. However, at higher frequencies, the supporting metal plate mainly functions like a reflector. As for antenna 1, strong radiation is also directed to the $+y$ direction at lower frequencies, while at higher frequencies, the radiation in the upper hemisphere is seen to be stronger. This behavior also suggests that the supporting metal plate functions like a radiator at lower frequencies and like a reflector at higher frequencies.

5. CONCLUSION

A small-size planar LTE/WWAN antenna and the antenna array formed using the same suitable for thin-profile tablet computer applications have been proposed. The antenna has a simple structure and is easy to implement by printing on a surface of a thin FR4 substrate. The total antenna size is only $10 \times 45 \text{ mm}^2$, yet it can provide two wide operating bands to cover the 704–960 and 1710–2690 MHz bands for LTE/WWAN operation. The antenna is a modified PIFA, and the applied bandwidth-enhancement techniques have been discussed in this study. In addition, because of the small size of simple structure of the proposed antenna, promising antenna arrays formed using the same have been studied. Over the operating bands, the antenna arrays show good isolation between the antennas and good radiation characteristics as well. The obtained results suggest that the proposed antenna and the antenna array formed using the same are promising for practical MIMO or dual talk (dual WWAN) operation in the thin-profile tablet computers.

REFERENCES

1. K.L. Wong and T.J. Wu, Small-size LTE/WWAN coupled-fed loop antenna with band-stop matching circuit for tablet computer, *Microwave Opt Technol Lett* 54 (2012), 1189–1193.
2. K.L. Wong, Y.C. Liu, and L.C. Chou, Bandwidth enhancement of WWAN/LTE tablet computer antenna using embedded parallel resonant circuit, *Microwave Opt Technol Lett* 54 (2012), 305–309.
3. T.W. Kang and K.L. Wong, Simple two-strip monopole with a parasitic shorted strip for internal eight-band LTE/WWAN laptop computer antenna, *Microwave Opt Technol Lett* 53 (2011), 706–712.
4. T.W. Kang, K.L. Wong, L.C. Chou, and M.R. Hsu, Coupled-fed shorted monopole with a radiating feed structure for eight-band LTE/WWAN operation in the laptop computer, *IEEE Trans Antennas Propagat* 59 (2011), 674–679.
5. K.L. Wong and P.J. Ma, Coupled-fed loop antenna with branch radiators for internal LTE/WWAN laptop computer antenna, *Microwave Opt Technol Lett* 52 (2010), 2662–2667.
6. T.W. Kang and K.L. Wong, Internal printed loop/monopole combo antenna for LTE/GSM/UMTS operation in the laptop computer, *Microwave Opt Technol Lett* 52 (2010), 1673–1678.
7. K.L. Wong and W.J. Lin, WWAN/LTE printed slot antenna for tablet computer application, *Microwave Opt Technol Lett* 54 (2012), 44–49.
8. Y.L. Ban, S.C. Sun, J.L.W. Li, and W. Hu, Compact coupled-fed wideband antenna for internal eight-band LTE/WWAN tablet computer applications, *J Electromagn Waves Appl* 26 (2012), 2222–2233.
9. S.H. Chang and W.J. Liao, A broadband LTE/WWAN antenna design for tablet PC, *IEEE Trans Antennas Propagat* 60 (2012), 4354–4359.
10. K.L. Wong, W.J. Wei, L.C. Chou, WWAN/LTE printed loop antenna for tablet computer and its body SAR analysis, *Microwave Opt Technol Lett* 53 (2011), 2912–2919.
11. C.L. Ku, W.F. Lee, and S.T. Lin, A compact slot inverted-F antenna to be embedded in the laptop computer for LTE/WWAN applications, *Microwave Opt Technol Lett* 53 (2011), 1829–1832.
12. D.L. Huang, H.L. Kuo, C.F. Yang, C.L. Liao, and S.T. Lin, Compact multibranch inverted-F antenna to be embedded in a laptop computer for LTE/WWAN/IMT-E Applications, *IEEE Antennas Wireless Propagat Lett* 9 (2010), 838–841.
13. K.L. Wong, Y.W. Chang, and S.C. Chen, Bandwidth enhancement of small-size WWAN tablet computer antenna using a parallel-resonant spiral slit, *IEEE Trans Antennas Propagat* 60 (2012), 1705–1711.
14. K.L. Wong and Y.C. Liu, Small-size WWAN tablet computer antenna with distributed and lumped parallel resonant circuits, *Microwave Opt Technol Lett* 54 (2012), 1348–1353.
15. Available at <http://www.ansys.com/products/hf/hfss/>, ANSYS HFSS Ansoft Corp., Pittsburgh, PA.
16. A. Andujar, J. Anguera, and C. Puente, Ground plane boosters as a compact antenna technology for wireless handheld devices, *IEEE Trans Antennas Propagat* 59 (2011), 1668–1677.

17. M. Martinez-Vazquez, O. Litschke, M. Geissler, D. Heberling, A. Martinez-Gonzalez, and D. Sanchez-Hernandez, Integrated planar multiband antennas for personal communication handsets, *IEEE Trans Antennas Propagat* 54 (2006), 384–391.
18. N. Lopez, C. Lee, A. Gummalla, and M. Achour, Compact metamaterial antenna array for long term evolution (LTE) handset application, *IEEE International Workshop on Antenna Technology (iWAT)*, Santa Monica, CA, 2009, pp. 1–4.
19. K.L. Wong, T.W. Kang, and M.F. Tu, Antenna array for LTE/WWAN and LTE MIMO operations in the mobile phone, *Microwave Opt Technol Lett* 53 (2011), 1569–1573.

© 2013 Wiley Periodicals, Inc.

A WIDE TUNING RANGE CMOS OSCILLATOR MIXER USING A PUSH-PUSH TECHNIQUE FOR V-BAND APPLICATIONS

Po-Yu Ke, Fan-Hsiu Huang, Hsuan-Lin Kao, and Hsien-Chin Chiu

Department of Electronics Engineering, Chang Gung University, Taoyuan, Taiwan, R.O.C; Corresponding author: hcchiu@mail.cgu.edu.tw

Received 3 January 2013

ABSTRACT: This work proposes a wide tuning oscillator mixer that operates from 56 to 64 GHz and is based on 90 nm CMOS technology. The circuit of a voltage control oscillator (VCO) comprises a mixer core and a coupled line marchand balun. The balanced mixer is symmetric, inherently broadband, and dependent on an LO balun that is combined with the parasitic capacitances from the mixer. The VCO is used in a 60 GHz push-pull circuit to generate the second harmonic, and a 30 GHz dielectric resonator is utilized to stabilize the fundamental oscillation frequency. The LC-tank oscillator also functions as a single-balanced LO load for the mixer core. A theoretical expression for the conversion gain of the self-oscillating mixer is given, taking into account the time-varying nature of the LO load impedance. Measurements show that the mixer has a conversion gain of 3.4 dB. Its output $P_{1\text{ dB}}$ is -12.4 dBm. The chip consumes 17.9 mW of dc power and it occupies an area of 0.64 mm^2 without pads. © 2013 Wiley Periodicals, Inc. *Microwave Opt Technol Lett* 55:1934–1937, 2013; View this article online at wileyonlinelibrary.com. DOI 10.1002/mop.27717

Key words: wide tuning; CMOS; mixer; push-push VCO

1. INTRODUCTION

The demand for a high data rate explains the massive interest in the unlicensed band, which has a large available bandwidth of 7 GHz (57–64 GHz in the USA, 59–66 GHz in Japan, and 57–66 GHz in Europe). This is supported by standards and applications that are led by such as WiHD, WiGig and 802.15c. Interest in IEEE802.15 communications systems for indoor and high-speed wireless applications has led to significant progress in broadband mmW integrated circuits and wireless personal area networks, the aim of which is to provide data rates of 2 to 3 Gbit/s or even higher.

Mixers and voltage control oscillator (VCO) are often designed in a modular fashion, meaning that, to a large extent, they are designed as isolated blocks that are eventually interconnected together. However, if the mixer and its VCO are viewed as an unified circuit, new and interesting design concepts emerge [1,2]. The resulting circuits are usually called self-oscillating mixers, or SOMs for short [3–5]. The SOMs' oscillator frequency tuning is determined by the variable device used in

the resonating tank, for instance, varactor diodes; varactor diodes commonly control the tuning range in a typical LC VCO. Therefore, in an LC VCO varactor size should be carefully chosen to maximize the tuning range. However, the parasitic parameters within the resonating tank elements seriously constrain the frequency tuning range. This limiting effect becomes more obvious as frequency increases [6–8].

This article proposes a new self-mixing technique that uses a mixer as a following stage of the push-push VCO core to generate the second harmonic. Therefore, the range of tunable frequencies in the desired frequency band is twice as wide as that available in the VCO core.

2. CIRCUIT DESIGN

Figure 1 shows the proposed functional block diagram. The second harmonic of the VCO output frequency is obtained and peaked at the common node of the cross-couple pair using the push-push technique. VCO can generate the second harmonic signals ($2F_{LO}$) with the differential harmonic signals ($+2F_{LO}$ and $-2F_{LO}$) at the output nodes of the balun. In the mixer circuit of the single-balance structure, accurate differential $2F_{LO}$ is generated in the local oscillator signal. The output signal of the down-conversion mixer is considered where the input RF signal is mixed by a LO signal and then an intermediate frequency (IF) is obtained at the output terminal.

Figure 2 shows the proposed circuit. To widen the range of operating frequencies and improve the phase noise performance following frequency mixing, the VCO must have a wide tuning range and favorable phase noise. The capacitance tuning ratio of a VCO can be expressed as [8].

$$\text{Tuning_Ratio} = \frac{C_{t,\text{max}} + C_{\text{fix}}}{C_{t,\text{min}} + C_{\text{fix}}} \quad (1)$$

Where $C_{t,\text{max}}$ and $C_{t,\text{min}}$ are the maximum and minimum varactor capacitances, respectively, and C_{fix} is the fixed parasitic capacitance. Based on Eq. (1), the frequency tuning range can be increased by either increasing the varactor capacitance or reducing the parasitic capacitance. A higher varactor capacitance typically results in degradation of the quality factor of the LC-tank. Therefore, in the proposed VCO design, the NMOS-only cross-coupled pair (M_1 – M_2) is adopted to generate negative resistance. Such an NMOS-only structure introduces less parasitic capacitances than the CMOS structure or the PMOS-only structure. The MOS varactor (C_v) of the accumulation-type provides the appropriate $C_{t,\text{max}}/C_{t,\text{min}}$ ratio (202fF/51fF) with a quality factor of 11.8–22.4 at 30 GHz, as shown in Figures 3(a) and 3(b). This particular topology requires a lower operating

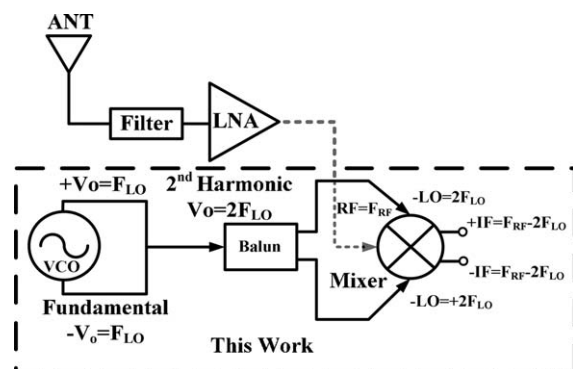


Figure 1 Function block diagram of our proposal circuits